

## Spatial inhomogeneities in iron pnictide superconductors: The formation of charge stripes

Lev P. Gor'kov

*NHMFL, Florida State University, 1800 East Paul Dirac Drive, Tallahassee Florida 32310, USA  
and L.D. Landau Institute for Theoretical Physics of the RAS, Chernogolovka 142432, Russia*

Gregory B. Teitel'baum\*

*E.K. Zavoiskii Institute for Technical Physics of the RAS, Kazan 420029, Russia*

(Received 22 June 2010; published 21 July 2010)

The heterogeneous coexistence of antiferromagnetism [spin-density wave (SDW)] and superconductivity on a mesoscopic scale was observed in iron pnictides in many recent experiments. We suggest and discuss the scenario in which the heterogeneity is caused by formation of domain walls inherent to the SDW state of pnictides at a proper doping or under applied pressure. Superconductivity would emerge from the modulated SDW structure. The phenomenon is akin to the Fulde-Ferrel-Larkin-Ovchinnikov (FFLO) phase in superconductors.

DOI: [10.1103/PhysRevB.82.020510](https://doi.org/10.1103/PhysRevB.82.020510)

PACS number(s): 74.25.Dw, 74.40.Kb, 74.70.Xa, 75.30.Fv

The new vast class of layered high- $T_c$  superconductors, iron pnictides,<sup>1</sup> manifests diverse and uncommon magnetic, structural, and superconducting properties.<sup>2</sup> Below we address competition between magnetism (SDW) and superconductivity (SC) that take place near the so-called “quantum critical point” (QCP) on the pnictides’ phase diagram tuned by either doping or pressure. In experiments<sup>3,4</sup> the competition assumes a form of the heterogeneous phase coexistence. We demonstrate that the heterogeneity can be due to the new SDW phase, where the staggered magnetization is modulated by the emergent periodic stripes, the lattice of solitons. In this vicinity SC arises on the background of the soliton phase (SP). Density of states (DOS) in SP has the same order of magnitude as in the paramagnetic (PM) phase.

Currently, the consensus is that the weak-coupling nesting model<sup>5</sup> correctly describes the most typical peculiarities of the pnictides’, at least qualitatively.

We confine ourselves to the picture of *only two* Fermi surfaces (FSs): the one for holes at the  $\Gamma$  point, (0,0) point and the other, for electrons, at the M point,  $(\pi, \pi)$ , in the folded Brillouin zone. The model is in broad use in the literature (see, for instance, in Ref. 6) and among other things reproduces the overall view of the phase diagram as a function of doping,<sup>6</sup> the interplay and the sequence of magnetic and structural transitions in the undoped compounds.<sup>7</sup> In particular, by way of changing the degree of nesting the model provides the built-in mechanism for the competition between magnetism and superconductivity at weak doping or under applied pressure.

Among many aspects of the original nesting model<sup>8</sup> that were recently investigated afresh in numerous theoretical papers, there exists one interesting feature that deserves more attention. The phenomenon consists in appearance of a spatially nonuniform SDW state in pnictides under rather general conditions near QCP.

Our attention to such a possibility was attracted by experiments.<sup>3,4</sup> In Ref. 4 a spontaneous spatial hybrid SDW/SC structure (of few nanometer) was reported in the  $\text{SrFe}_2\text{As}_2$  crystal under pressure. In Ref. 3 the heterogeneous phase coexistence was observed in single underdoped  $(\text{Ba, K})\text{Fe}_2\text{As}_2$  crystal both above and below SC  $T_c$ . The spatial scale in Ref. 3 amounted to 65 nm.

In the scenario under investigation the tendency to form the periodic domain structure is inherent into the SDW nesting mechanism itself. Therefore, onset of the modulated SDW phase may occur at temperatures even above SC  $T_c$ . Precisely such behavior was found in the quasi-one-dimensional Bechgaard salt,  $(\text{TMTSF})_2\text{PF}_6$ .<sup>9</sup> The modulated SDW (at a fixed pressure,  $P < P_{cr}$ , i.e., before QCP) was seen above and below the transition into the new SC state and interpreted in terms of the new ground state: SP.<sup>10</sup>

First, as it seems, modulated charge-density wave (CDW) or SDW phases in three dimensions were discussed in Refs. 11 and 12. In Ref. 12 the authors investigated the model<sup>8</sup> of the two anisotropic FS with the shapes deviating from the perfect nesting. Consequently, the energy spectrum for electron and holes was chosen as  $H_{e,h} = \pm v_{F1,2}[t - \eta_{1,2}(\vec{p})]$ , correspondingly ( $t$  is the momentum component normal to FS). Deviations from the ideal nesting  $\eta_1(\vec{p})$  and  $\eta_2(\vec{p})$  describe both the anisotropy and the doping.

Analysis<sup>12</sup> had shown that the instability line with respect to transition into a *commensurate* CDW (or SDW) phase in the  $(T, \eta)$  plane possesses the reentrant character, similar to a superconductor placed into the exchange field,  $I\sigma_z$ .<sup>13,14</sup> On the side of large (antinesting) terms,  $\eta_1(\vec{p})$  and  $\eta_2(\vec{p})$ , the onset of SDW first occurs at an incommensurate (IC) vector  $\vec{Q} = \vec{Q}_0 + \vec{q}$ , where  $\vec{Q}_0(\pi, \pi)$  is the commensurate vector at zero  $\eta_1(\vec{p})$ ,  $\eta_2(\vec{p})$ . At  $T=0$  the  $\vec{q}$  vector is related to the magnitude and the anisotropy combined, as given by the antinesting factor,  $|\eta_1(\vec{p}) - \eta_2(\vec{p})|$  (Ref. 12)

$$\left\langle \ln \left[ |(\eta_1 - \eta_2)^2 - (\cos \varphi)^2 q^2| \left( \frac{2v_{F1}v_{F2}\gamma}{\pi T_{c0}(v_{F1} + v_{F2})} \right)^2 \right] \right\rangle = 0, \quad (1)$$

where  $T_{c0}$  is the temperature of SDW onset at the ideal nesting,  $\varphi$  is the angle between  $\vec{q}$  and the normal vector to FS, and  $\gamma=1.781$  is the Euler constant. Average,  $\langle \dots \rangle$ , is taken along FS.

Appearance of an IC SDW on the phase diagram of pnictides was discussed earlier (see, for instance, Refs. 6 and 15). However, we emphasize the profound difference between IC SDW and the inhomogeneous SDW state, where electronic

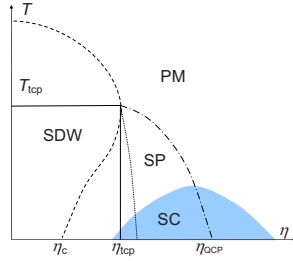


FIG. 1. (Color online) The  $(T, \eta)$  phase diagram ( $\eta$ -tuning parameter): the instability line (dashed) for commensurate SDW shows reentrance below the tricritical point  $(T_{tcr}, \eta_{tcr})$ ; SP starts before the putative first-order transition line (dotted) and extends to the PM phase boundary (dashed-dotted). The QCP is covered by the SC dome. See text for details.

degrees of freedom inside domain walls (DWs) are not gapped which leads to a finite and spatially inhomogeneous DOS (see below).

On the  $(T, \eta)$ -phase diagram in Fig. 1 the instability line (dashed) for the commensurate SDW ( $\vec{q}=0$ ) displays reentrance below the tri-critical point  $(T_{tcr}, \eta_{tcr})$ ; the dotted line that goes down from the same point is the would-be line of the first-order transition between the commensurate SDW and the paramagnetic phase. The periodic SP supersedes this transition. The new phase extends to the dashed-dotted line on the right. The position of the QCP *inside* the SC dome is shown tentatively.

We derive the system of the Eilenberger-type equations describing the inhomogeneous SP state. With the view to demonstrate the distinct phenomenon, we accept the model<sup>12</sup> assuming a density-density interaction between the  $e$  and  $h$  pockets. The analytical solution for SP is not available. In particular, if the ideal nesting is broken by *doping only*, the substitution,  $v_F \eta_1(\vec{p}) = -v_F \eta_2(\vec{p}) = \text{const} \Rightarrow I$ , leads to equations identical to the ones for FFLO problem,<sup>13,16</sup> solved numerically in Ref. 17. Same methods apply to the equations for Fe pnictides in the general case. Later on in the Rapid Communication, we investigate emergence of domains from the homogeneous SDW/CDW state at the increasing strength of the parameters,  $\eta_1(\vec{p})$ ,  $\eta_2(\vec{p})$ , say, by pressure.

Derivation of the Eilenberger-style equations for the itinerant three-dimensional or two-dimensional (2D) SDW/CDW case is similar to their original derivation<sup>18</sup> from the Gor'kov equations in superconductors and is described below only briefly. (Similar equations were used for one-dimensional physics in Ref. 19.)

Introduce the matrix Green's function

$$\hat{G}(x, x') = \begin{pmatrix} G_{11} & G_{12} \\ -G_{21} & -G_{22} \end{pmatrix}. \quad (2)$$

Here  $G_{ik}(x, x') = \langle T(\bar{\psi}_i(x) \bar{\psi}_k^\dagger(x')) \rangle$ ,  $x = (\vec{r}, \tau)$ , and the nondiagonal indices, 12, 21, belong to the off-diagonal Green's functions, nonzero in the presence of SDW/CDW order. The two FSs are connected by the structure vector  $\vec{Q}$ . To save on the notations, we consider the CDW case. The only difference is in the spin matrix,  $(\vec{\sigma} \cdot \vec{l})$ , present as a factor, in the definitions of the nondiagonal SDW components,  $G_{i \neq k}(x, x')$  ( $\vec{l}$  stands

for the staggered magnetization directed along one of the axes in  $ab$  plane).

We then write down the first pair of equation

$$(\partial/\partial\tau + \hat{H}_e)G_{11}(x, x') + \Delta_{\vec{Q}}(\vec{r})G_{21}(x, x') = 1,$$

$$(\partial/\partial\tau + \hat{H}_h)G_{21}(x, x') + \Delta_{-\vec{Q}}^*(\vec{r})G_{11}(x, x') = 0. \quad (3)$$

Here

$$\Delta_{\vec{Q}}(\vec{r}) \equiv \lambda G_{21}(\vec{r}; \tau_1 = \tau_2); \quad \Delta_{-\vec{Q}}^*(\vec{r}) \equiv \lambda G_{12}(\vec{r}; \tau_1 = \tau_2). \quad (4)$$

( $\lambda$  is proportional to the interaction constant.)

To account for the spatial dependence in Eq. (4), we write for free electrons and holes ( $\mu$  is the chemical potential)

$$\hat{H}_{e,h} = \mp (\nabla^2/2m_{1,2} + \mu) \mp v_{F1,2} \cdot \eta_{1,2}(\vec{p}). \quad (5)$$

The “gap” parameters [Eq. (4)] couple the electron and the hole FSs. Following Ref. 18, introduce the operator in the left-hand side of Eq. (3),

$$\check{G}_L^{-1} = \begin{pmatrix} \partial/\partial\tau + \hat{H}_e & -\Delta_{\vec{Q}}(\vec{r}) \\ \Delta_{-\vec{Q}}^*(\vec{r}) & -\partial/\partial\tau - \hat{H}_h \end{pmatrix} \quad (6)$$

so that  $\check{G}_L^{-1} \times \hat{G}(x, x') = \delta(x - x')$ . The operator that acts on the matrix [Eq. (2)] from the right side:  $\hat{G}(x, x') \times \check{G}_R^{-1} = \delta(x - x')$  is obtained by changing  $\partial/\partial\tau \rightarrow -\partial/\partial\tau$ .

Substitute  $\partial/\partial\tau \Rightarrow -i\omega_n$  in  $\check{G}_L^{-1}$  and  $\partial/\partial\tau \Rightarrow +i\omega_n$  in  $\check{G}_R^{-1}$  and rewrite equations for the frequency Fourier components. The Green's functions are not diagonal in the momentum representation

$$\hat{G}(x, x') \Rightarrow \hat{G}(\omega_n; \vec{r}, \vec{r}') \Rightarrow \hat{G}(\omega_n; \vec{p}, \vec{p} - \vec{k}). \quad (7)$$

The essence of the “quasiclassical” method<sup>18,20</sup> in the theory of superconductivity is in integrating out the energy variable  $\xi_{\vec{p}} = v_F t \equiv v_F(p - p_F)$  thus, rewriting equations in terms of new functions

$$\int \frac{d\xi_{\vec{p}}}{i\pi} \hat{G}(\omega_n; \vec{p}, \vec{p} - \vec{k}) \Rightarrow \hat{g}(\omega_n; \vec{p}_F, \vec{k}) \equiv \begin{pmatrix} g_{11}(\omega_n; \vec{p}_F, \vec{k}) & g_{12}(\omega_n; \vec{p}_F, \vec{k}) \\ -g_{21}(\omega_n; \vec{p}_F, \vec{k}) & -g_{22}(\omega_n; \vec{p}_F, \vec{k}) \end{pmatrix}. \quad (8)$$

In a superconductor, the characteristic scale for  $T_c$ 's is usually much less than the energy Fermi:  $T_c \ll E_F$ . With the characteristic scale for the magnetic transition,  $T_{SDW} \sim 100-200$  K and the Fermi pockets energy scale  $\sim 0.2$  eV,<sup>2</sup> the quasiclassical approach is expected to work well enough for pnictides as well.

The equations for the integrated Green's function in Refs. 18 and 20 emerge from commuting the matrix equations for the Green's functions:  $\check{G}_L^{-1} \times \hat{G} - \hat{G} \times \check{G}_R^{-1} = 0$  from whence the variable  $\xi_{\vec{p}}$  drops out. Omitting the arguments of  $\hat{g}(\omega_n; \vec{p}_F, \vec{k})$  and denoting  $\delta_{\vec{p}_F} = v_F[\eta_1(\vec{p}_F) - \eta_2(\vec{p}_F)]$ , the resulting equations acquire the form

$$-i(\vec{v}_F \cdot \vec{V})g_{11} + \Delta_{\vec{Q}}(\vec{r})g_{21} - \Delta_{-\vec{Q}}^*(\vec{r})g_{12} = 0,$$

$$\{-i(\vec{v}_F \cdot \vec{\nabla}) - 2i\omega_n - \delta_{\vec{p}_F}\}g_{12} + 2\Delta_{\vec{Q}}(\vec{r})g_{11} = 0,$$

$$\{+i(\vec{v}_F \cdot \vec{\nabla}) - 2i\omega_n - \delta_{\vec{p}_F}\}g_{21} + 2\Delta_{-\vec{Q}}^*(\vec{r})g_{11} = 0. \quad (9)$$

As in Ref. 18,  $g_{11}=g_{22}$  and the normalization condition is  $g_{11}^2 - g_{12}g_{21} = 1$ . The self-consistent Eq. (4) now is

$$\Delta_{\vec{Q}}(\vec{r}) = \lambda T \int dS_{\vec{p}_F} \sum_n g_{21}(\omega_n; \vec{p}_F, \vec{k}). \quad (10)$$

Equations (9) and (10) form the closed system. (One drawback of the quasiclassical method is that at the derivation one needs  $v_{F1}=v_{F2}$ ,  $m_1=m_2$ .) In Fe pnictides two FSs are connected by the commensurate vector  $\vec{Q}_0(\pi, \pi)$ . Therefore,  $\Delta(r)$  is real and we omit the index  $\vec{Q}$  below.

Parameters  $\eta$  depend on the specific material. Therefore, we stay below only on the principal properties of the SP. Near the right boundary of the area on the phase diagram in Fig. 1 occupied by SP, the amplitude of the SDW parameter,  $\Delta$ , is small and the periodic solution of the form  $\Delta(r) = \Delta \cos(\vec{q}\vec{r})$  can be constructed by perturbations in Eqs. (3) and (4).<sup>12,13</sup> With the decrease in the  $\eta$  parameters and entering the developed SP, the period gradually increases; below a threshold at a critical value of the  $\eta$  parameters, the system enters the homogeneous SDW phase. Slightly above the threshold the structure consists of the almost isolated domains.

It presents the decided interest to consider formation of one single DW at the threshold as it sheds more light on peculiarities of SP. Assume the dependence of  $\Delta(x)$  on one spatial variable. Return to Eq. (3) and address the problem of the eigenvalues and the two-component eigenfunctions  $(u, v)$  for their left-hand sides ( $\partial/\partial\tau \Rightarrow -E$ )

$$\begin{aligned} [-iv_{F,x} \partial/\partial x - v_F \eta_1(\vec{p}_F)]u + \Delta(x)v &= E(v_{F,x}, \vec{p}_F)u, \\ [+iv_{F,x} \partial/\partial x + v_F \eta_2(\vec{p}_F)]v + \Delta(x)u &= E(v_{F,x}, \vec{p}_F)v. \end{aligned} \quad (11)$$

The substitution  $u, v \Rightarrow (\bar{u}, \bar{v}) \times \exp(i[\frac{v_F}{2v_{F,x}}(\eta_1 + \eta_2)]x)$  transforms Eq. (11) into

$$\begin{aligned} -iv_{F,x} \partial \bar{u}/\partial x + \Delta(x)\bar{v} &= \tilde{E}(v_{F,x})\bar{u} \\ +iv_{F,x} \partial \bar{v}/\partial x + \Delta(x)\bar{u} &= \tilde{E}(v_{F,x})\bar{v}, \end{aligned} \quad (12)$$

where  $\tilde{E}(v_{F,x}) = E(v_{F,x}, \vec{p}_F) + \delta_{\vec{p}_F}/2$ .

Consider the energy spectrum for system [Eqs. (12)] in the presence of a rarified periodic array of DW. Near the isolated wall choose the gap,  $\Delta(x)$ , in the form (the correlation length  $\xi_0$  will be determined below)

$$\Delta(x) = \Delta_0 \cdot \tanh[x/(a\xi_0)]. \quad (13)$$

The distortion to the homogeneous state [ $\Delta(x) \equiv \Delta_0$ ] thus produced, is energetically unfavorable. At large separation between the walls the resulting energy loss is the sum of contributions originated near each domain,  $\Sigma E_s$ . (Here  $E_s$  is the one wall energy cost per unit length.)

Return now to the putative first-order transition shown in Fig. 1. To the homogeneous SDW/CDW phase corresponds the gain in the free-energy density:  $\Delta F_{\text{SDW}} = -2\nu(\varepsilon_F)\Delta_0^2$ , where  $\nu(\varepsilon_F) = m/4\pi$  is DOS per single spin. But deforma-

tions,  $\eta_1$  and  $\eta_2$ , of the two initially congruent FSs also decrease the energy of the normal (PM) state

$$\Delta F_n = -2\nu(\varepsilon_F)[\langle(v_F \eta_1)^2\rangle + \langle(v_F \eta_2)^2\rangle]. \quad (14)$$

Hence, if, for instance, the system is doped, the last mechanism may offset the energy cost,  $E_s > 0$ , of forming single DW owing to the fact that there are locally gapless states inside the wall in the form [Eq. (13)]. With previous parametrization of doping,  $v_F \eta_1 = -v_F \eta_2 = I$ , one can write the local PM contribution of Eq. (14) in the form

$$\Delta F_n(x) = -4\nu(\varepsilon_F)\bar{v}(x/x_0)I^2, \quad (15)$$

where  $x_0$  is a scale for the domain width. Denote by  $F_n^*(I)$  the integrated contribution from one single domain (per unit wall length):  $-F_n^* = -4\nu(\varepsilon_F)I^2 \int \bar{v}(x/x_0)dx$ . The threshold value,  $I_c$ , is determined by

$$E_s - F_n^*(I_c) = 0. \quad (16)$$

At  $I > I_c$  the spontaneous formation of domains will be arrested by their interactions.

In principle, finding  $E_s$ ,  $\bar{v}(x/x_0)$ , and the very profile of  $\Delta(x)$  [Eq. (13)] can be reduced to the self-consistent mean-field problem by solving Eqs. (12) for the band-energy spectrum and the eigenfunctions in the periodic potential,  $\Delta(x+L) = \Delta(x)$ . Near the wall where  $\Delta(x)$  has the form [Eq. (13)], Eq. (12) at  $L \gg x_0$  can be solved in terms of the hypergeometric functions. However, the need to account the periodicity of  $(\bar{u}, \bar{v})$  at large separations between walls makes the approach rather cumbersome.

With our main goal to attract attention to this phenomenon we choose the model<sup>12</sup> that allows the one-to-one mapping on the FFLO problem. Therefore, it is possible to avoid these tiresome calculations by instead making the use of the numerical results.<sup>17</sup> Without staying on further details, we obtained for  $\bar{v}(x/\xi_0) \approx 1.2ch^{-1}(0.63x/\xi_0)$ . Note that  $\bar{v}(x/\xi_0) \sim 1$  for  $x$  on the order of  $\xi_0$ , i.e., local DOS inside domain has the same order of magnitude as in the PM normal phase. That is also true in the periodic soliton lattice. With  $I_c = 0.655\Delta_0$  we found from Eq. (16) the soliton energy

$$E_s = 10.27 \cdot \nu(\varepsilon_F)\xi_0\Delta_0^2 = 0.26 \cdot p_F\Delta_0 \quad (17)$$

(we accepted the BCS value  $\xi_0 = \hbar v_F / \pi \Delta_0$ . The Planck's constant  $\hbar$  is restored in the expressions for  $\xi_0$ ).

With the soliton energy known, Eq. (17), turn now to the role of the anisotropy. Assume  $\int \delta(\vec{p}_F)dl_F \equiv 0$ , the equal numbers of electron and holes. Coming back to the relation between  $\tilde{E}(v_{F,x})$  and  $E(v_{F,x}, \vec{p}_F)$  in Eqs. (11) and (12), one sees that the energy spectrum of Eq. (12) for  $(\bar{u}, \bar{v})$  is pertinent only to distorted homogeneous phase, when negative contributions of the form of Eq. (15) are absent. The energy spectrum of Eq. (12), hence, contributes only to calculations of the soliton energy  $E_s$ . Account of the  $\delta_{\vec{p}_F}$  terms,  $E(v_{F,x}, \vec{p}_F) = \tilde{E}(v_{F,x}) - \delta_{\vec{p}_F}/2$ , decreases the cost of the single wall by filling up the momentum states with  $\delta_{\vec{p}_F} > 0$

$$E_{\text{kin}} = -2 \int \frac{dl_F}{2\pi} |\delta_{\vec{p}_F}|/2. \quad (18)$$

In the notations  $t(p_{\parallel}) \equiv \delta_{\vec{p}_F}/2$ ,  $p_{\parallel} = p_F \cos \alpha$ ,  $t(p_{\parallel})$  now defines the energy spectrum for carriers moving inside the wall. For

the corresponding DOS  $\nu_w(\varepsilon)$  (per single spin, per unit length) one has

$$\nu_w(\varepsilon) = \int \delta[\varepsilon - t(p_{\parallel})] dp_{\parallel} / 2\pi. \quad (19)$$

By the order of magnitude  $\nu_w(\varepsilon) \sim [dt(p_{\parallel})/dp_{\parallel}]^{-1} \sim p_F/t$ ; with  $t \sim \Delta_0$ ,  $\nu_w(\varepsilon) \sim p_F/\Delta_0$ . The DOS in Eq. (19) is concentrated inside the domain width  $\sim \xi_0$ . Therefore, the local DOS in the periodic soliton lattice with  $L \sim \xi_0$  is large, i.e., again of the same order as  $\nu(\varepsilon_F) = m/4\pi$  the 2D DOS in PM state.

Thus  $E_{kin} = E_s$  determines the threshold for onset of the modulated SDW state at large enough geometric mismatch between the two FS's. [The mechanism is akin to the one for forming periodic domains in  $(\text{TMTSF})_2\text{PF}_6$ .<sup>9,10,21</sup>]

Up to this point we studied only the variation in the SDW state with changes to the degree of nesting. Meanwhile, reducing the SDW gap also opens way to emergence of a SC phase. Interactions responsible for the first-order magnetic and structural transition seem to be stronger than the ones that lead to the SC pairing. Indeed, in the stoichiometric pnictides the former occurs at higher temperatures. In the area of the phase diagram discussed so far SC would develop on the background of the SP. Note that when SC is still weak, its appearance may not fully remove remnant DOS that, as we seen above, has by order of magnitude the same value as in PM state. This may explain the substantial residual density of states toward 0 K, revealed via nuclear spin-lattice relaxation rate in SC domains of  $\text{SrFe}_2\text{As}_2$  (Ref. 4) and via the finite linear coefficient in the specific heat in SC state.<sup>22</sup>

The heterogeneous phase coexistence reported in experiments<sup>3</sup> seems to realize the discussed scenario. Indeed, in Ref. 3 the heterogeneous state first sets in below  $T_{\text{SDW}} \approx 70$  K, i.e., well above  $T_c \approx 32$  K. While the magnetic force microscope (MFM) images do not visualize a period-

icity in some special direction, this, actually, is not expected. Below the first-order transitions samples are twinned. In addition, unlike the strongly anisotropic  $(\text{TMTSF})_2\text{PF}_6$ ,<sup>9</sup> the spontaneous formation of domains in pnictides can emerge along any arbitrary direction leading to a pattern similar to the one seen in Ref. 3. The similar sequence of phase transitions was observed in <sup>75</sup>As NMR studies of  $\text{BaFe}_2\text{As}_2$  doped by small amount of Co.<sup>23</sup> More recently, the scanning-force microscopy (SFM) measurements<sup>24</sup> in  $\text{CaFe}_{1.94}\text{Co}_{0.06}\text{As}_2$  revealed the existence of striped electronic nanostructures with dimensions  $\sim 4$  nm. Characteristic spatial scale for the superstructure is  $\xi_0 \sim 0.18\hbar v_F/T_{\text{SDW}}$  as obtained above. With the typical  $v_F \sim 10^7$  cm/s and  $T_{\text{SDW}} \sim 100$  K for pnictides it leads to few nanometer. The  $\mu\text{SR}$  measurements<sup>25</sup> were capable to determine only the volume fractions of the coexisting SDW and SC subphases. The hybrid SDW/SC structure found in Ref. 4 may correspond to the case when  $T_{\text{SDW}}$  is low and close to  $T_c$ , but we have no results when SDW and SC compete for existence on equal terms, i.e., under the SC dome near QCP in Fig. 1. Such a competition remains the subject of the great interest (see, e.g., Refs. 6 and 26).

To conclude, we have shown that emergence of a heterogeneous state with large local DOS is an intrinsic property of iron pnictides at low temperatures. Mechanisms of formation of a single DW near the threshold were investigated unveiling the difference in the role of doping and anisotropy. Although the simple model<sup>12</sup> omits many details concerning the interactions and the energy spectrum in real materials, it seems to confirm the view that mesoscopic phase separation observed by means of NMR,  $\mu\text{SR}$ , MFM, and SFM, in reality is nothing but the formation of the system of stripes.<sup>27</sup>

The work of L.P.G. was supported by the NHMFL through NSF Grant No. DMR-0654118 and the State of Florida, that of G.B.T. through the RFBR under Grant No. 10-02-01056.

\*grteit@kfti.knc.ru

<sup>1</sup>Y. Kamihara *et al.*, *J. Am. Chem. Soc.* **130**, 3296 (2008).

<sup>2</sup>*Physica C* **469**, 313 (2009), special issue on superconductivity in iron pnictides.

<sup>3</sup>J. T. Park *et al.*, *Phys. Rev. Lett.* **102**, 117006 (2009).

<sup>4</sup>K. Kitagawa *et al.*, *Phys. Rev. Lett.* **103**, 257002 (2009).

<sup>5</sup>D. Singh *et al.*, *Physica C* **469**, 886 (2009).

<sup>6</sup>M. Vavilov *et al.*, *Supercond. Sci. Technol.* **23**, 054011 (2010); A. B. Vorontsov *et al.*, *Phys. Rev.* **79**, 060508(R) (2009).

<sup>7</sup>V. Barzykin and L. P. Gor'kov, *Phys. Rev. B* **79**, 134510 (2009).

<sup>8</sup>L. V. Keldysh and Yu. V. KopaeV, *Sov. Phys. Solid State* **6**, 2219 (1965); A. N. Kozlov and L. A. Maksimov, *Sov. Phys. JETP* **22**, 889 (1966).

<sup>9</sup>B. Salameh *et al.*, *Physica B* **404**, 476 (2009); N. Kang *et al.*, *Phys. Rev. B* **81**, 100509(R) (2010).

<sup>10</sup>L. P. Gor'kov and P. D. Grigoriev, *Europhys. Lett.* **71**, 425 (2005).

<sup>11</sup>T. M. Rice, *Phys. Rev. B* **2**, 3619 (1970).

<sup>12</sup>L. P. Gor'kov and T. T. Mnatzakanov, *Sov. Phys. JETP* **36**, 361 (1973).

<sup>13</sup>A. I. Larkin and Y. N. Ovchinnikov, *Sov. Phys. JETP* **20**, 762 (1965).

<sup>14</sup>L. P. Gor'kov and A. I. Russinov, *Sov. Phys. JETP* **19**, 922 (1964).

<sup>15</sup>V. Cvetkovic and Z. Tesanovic, *Phys. Rev. B* **80**, 024512 (2009).

<sup>16</sup>P. Fulde and R. A. Ferrell, *Phys. Rev.* **135**, A550 (1964).

<sup>17</sup>H. Burkhardt and D. Rainer, *Ann. Phys.* **506**, 181 (1994).

<sup>18</sup>G. Eilenberger, *Z. Phys.* **214**, 195 (1968).

<sup>19</sup>S. N. Artemenko and A. F. Volkov, in *Charge Density Waves in Solids*, edited by L. Gor'kov and G. Grüner (Elsevier Science, Amsterdam, 1989), Chap. 9.

<sup>20</sup>A. I. Larkin and Yu. N. Ovchinnikov, *Sov. Phys. JETP* **28**, 1200 (1969).

<sup>21</sup>S. A. Brazovskii *et al.*, *Phys. Scr.* **25**, 423 (1982).

<sup>22</sup>F. Hardy *et al.*, *Phys. Rev. B* **81**, 060501(R) (2010).

<sup>23</sup>M.-H. Julien *et al.*, *EPL* **87**, 37001 (2009).

<sup>24</sup>T.-M. Chuang *et al.*, *Science* **327**, 181 (2010).

<sup>25</sup>T. Goko *et al.*, *Phys. Rev. B* **80**, 024508 (2009).

<sup>26</sup>M. Bendele *et al.*, *Phys. Rev. Lett.* **104**, 087003 (2010).

<sup>27</sup>We believe that our model of doping the AFM state in the case of the two exactly nested FSs would be in the close analogy to the stripe formation in cuprates after accounting for the long-range Coulomb interactions. The latter are usually screened in iron pnictides.